An Elasticity Model Considering Grain Boundaries and Tensile Orientations for Directionally Solidified Superalloys

XIAO Jianfeng, ZHANG Hongjian, WEN Weidong, CUI Haitao*

Aero-engine Thermal Environment and Structure Key Laboratory of Ministry of Industry and Information Technology;
Jiangsu Province Key Laboratory of Aerospace Power System;
State Key Laboratory of Mechanics and Control of Mechanical Structures;
College of Energy & Power Engineering, Nanjing University of Aeronautics and Astronautics, Nanjing 210016, P.R. China

(Received 10 April 2018; revised 25 December 2018; accepted 27 April 2019)

Abstract: In order to investigate the elastic properties of directionally solidified (DS) superalloys, an elasticity model called boundaries elastic model (GBE model), considering grain boundaries and tensile orientations, is proposed in this paper. Two assumptions are adopted in the GBE model: (1) The displacement of grains, which moves along the perpendicular direction, is restricted by the grain boundaries; (2) Grain boundaries influence region (GBIR) is formed around the grain boundaries. Based on the single crystal (SC) calculation method of elastic properties, the GBE model can well predict macroscopic equivalent elastic modulus (Young's modulus) of DS superalloys under different tensile orientations effectively. To demonstrate the correctness of the GBE model, 3D finite element simulation is adopted and tensile experiments on a Ni_3Al-base DS superalloy (IC10) along five tensile orientations are carried out. Meanwhile, the grain boundaries are observed by light microscopy and transmission electron microscope (TEM). Therefore, the GBE model is proved to be feasible by comparing the simulated results with the experiments.

Key words: directionally solidified superalloys; single crystal; Young's modulus; grain boundaries

CLC number: V252.2 **Document code**: A **Article ID**: 1005-1120(2019)04-0652-11

0 Introduction

Directionally solidified (DS) superalloys have been greatly developed to meet the requirements of increasing turbine inlet temperature of gas turbine engines. The typical features of DS superalloys are that the transverse grain boundaries are eliminated and the growth directions of grains can be controlled to get paralleled grains[1-4]. DS superalloys are a class of materials with a controlled grain growth direction and the grains in DS superalloys parallel to each other[1-4]. As grain growth direction parallels to that of the maximum principal stress, mechanical properties of DS superalloys are better than polycrystals with randomly oriented grain boundaries[5]. In recent years, although more and more studies have been implemented on the macro or micro behaviors of single crystals and polycrystals[6-8], the properties of DS superalloys have hardly been addressed. Misra et al.[9], Asthana et al.[10] and Bei et al.[11] investigated different DS superalloy systems to determine the effects of microstructure on mechanical properties; Sai et al.[12], Shi et al.[13] and Shenoy et al.[14] studied the unidirectional mechanical behavior, the creep behavior and the thermal mechanical fatigue of DS superalloys, respectively; finite element (FE) structure computations were introduced to develop a multi-scale model on DS superalloys by Martin et al.[15]. Meanwhile, a lot of studies on the microstructures, the uniaxial tensile mechanical behaviors and the yield properties under biaxial tension have been conducted on IC10 alloy, which is a typical Ni3Al-base DS superalloy in Chi-

*Corresponding author, E-mail address: zhanghongjian@nuaa.edu.cn.

How to cite this article: XIAO Jianfeng, ZHANG Hongjian, WEN Weidong, et al. An Elasticity Model Considering Grain Boundaries and Tensile Orientations for Directionally Solidified Superalloys[J]. Transactions of Nanjing University of Aeronautics and Astronautics, 2019,36(4):652-662.
http://dx.doi.org/10.16356/j.1005-1120.2019.04.012

na[16-19]. In these studies, the elastic properties of DS superalloys are almost obtained from the experimental analyses[13-14] and the calculations based on the empirical formulation of single crystals[20]. Five elastic constants need to be addressed in the experimental analyses, which will increase the experimental cost. However, in the later method, if the tensile orientation is far away from the grain growth direction, the differences of the elastic constants between single crystals and DS superalloys are obvious. Thus, this method has the demerit of small applicable range.

Recently, the most commonly used methods for predicting the elastic properties for polyorystals are based on the Voigt and Reuss average assumptions[21]. When using the concept of Voigt average, it is assumed that the strain in each grain of the alloy is the same. However, the uniformity of stress in all grains is introduced to the Reuss average assumption. In this way, the macroscopic elastic stiffness is obtained from the volume average of the stiffness in all grains. The Voigt method gives an upper bound of elastic stiffness, while the Reuss method gives the lower bound. Although these approaches are simple and effective for polycrystals, they are unable to account for some important features for DS superalloys, such as the growth direction of grains and the effects of grain boundaries. Subsequently, Yaguchi et al.[5] developed an elastic formation from the self-consistent method based on the mean field theory. The orientations of grains were detected by electron back scatter diffraction (EBSD) technology, while the influence of grain boundaries on the deformation of DS superalloys had not been considered. Simultaneously, repeated iterations were essential in this study, which were inconvenient in engineering application. In addition, the elastic properties of DS superalloys were the building blocks of other mechanical properties, such as intensive and fatigue properties. Therefore, a simple approach to acquire the elastic properties of DS superalloys is urgent.

As is known to all, the most significant difference between the single crystals and the DS superalloys is grain boundaries. In the past few decades, a mass of studies[6-8,22-23] have been conducted on single crystals and several empirical formulae have been proposed to predict the elastic constants of single crystals[22]. On the basis, an elastic formulation for DS superalloys will be established, inspired by Yaguchi's work and Voigt's method. This model considers grain boundaries and tensile orientations, and defined as the grain boundary elastic model (GBE model) based on the empirical formula of single crystals. There are only two model parameters need to be addressed. Therefore, it costs less than determining five parameters. Furthermore, in order to prove the correctness and effectiveness of GBE model, experiments on IC10 DS are implemented and FE simulations is conducted. Finally, the macroscopic equivalent elastic modulus of IC10 DS predicted by different approaches (GBE model, experiments and FE simulations) are compared and discussed together.

1 Development of GBE Model for DS Superalloys

Considering the influences of grain boundaries and loading directions for DS superalloys, two assumptions are adopted in the GBE model: (1) The displacement of grains, which moves along the perpendicular direction, is restricted by the grain boundaries; (2) grain boundary influence region (GBIR) is formed around the grain boundaries and the width of GBIR is several times of that of the grain boundaries.

1.1 Microstructures of DS superalloys

As is well known, the directional solidification technique can well eliminate transversal grain boundaries, thus forming orderly arranged column crystals. These column crystals present nearly identical growth direction, while random orientations in the plane are perpendicular to the growth direction, as shown in Fig.1(a). For simplicity, grains in DS superalloy could be considered as idealized cylinders,

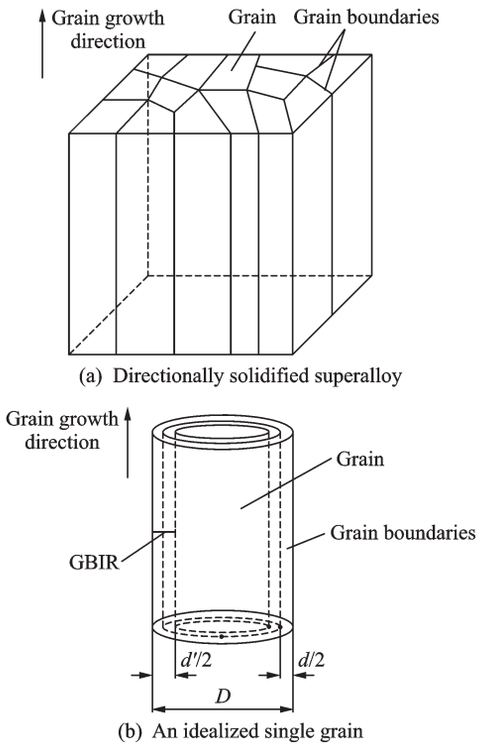

Fig.1 Schematics of grain morphologies

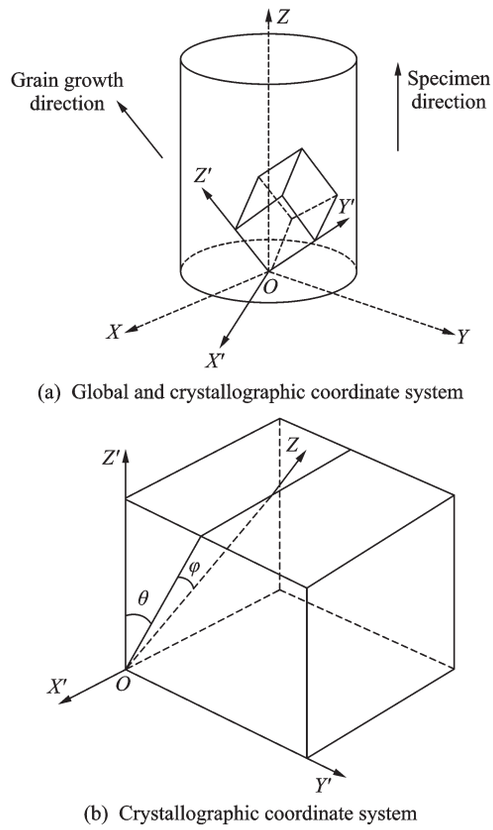

Fig.2 Relationship between different coordinate systems

shown in Fig.1(b), where D, d and d' are the diameter of one grain, the width of the grain boundary and the width of the GBIR, respectively.

1.2 Elastic formulation inside grain

In this paper, it is assumed that the elastic formulation inside the grain is the same as that of single crystals (SC). Thus, elastic formulation of SC is summed up here. As single crystal is anisotropic, elastic properties along different loading directions are not identical. Meanwhile, because of the cubic structure of single crystal, the properties along each principle axes of material are supposed to be identical. Furthermore, to depict the stiffness model of single crystal clearly, two coordinate systems will be used, such as the global system and the crystallographic system. Usually, one axis in global coordinate system coincides with a test specimen axis or the loading direction, while one axis in crystallographic coordinate system coincides with the growth direction of the grain. The relationship between two systems are shown in Fig.2(a) where system X-Y-Z is a global coordinate system and X'-Y'-Z' is a crystallographic coordinate system, θ and ψ are the Euler angles, as shown in Fig.2(b).

Usually, the stress-strain relationship of single crystals in the crystallographic coordinate system can be defined as

$$\{\boldsymbol{\sigma}\} = \boldsymbol{D}\{\boldsymbol{\varepsilon}\} \tag{1}$$

where $\{\boldsymbol{\sigma}\}$ and $\{\boldsymbol{\varepsilon}\}$ are 6×1 stress and strain vectors in crystallographic coordinate system, respectively, and $\boldsymbol{D}$ is a 6×6 stiffness matrix in crystallographic coordinate system, expressed in

$$\boldsymbol{D} = \begin{bmatrix} D_{11} & D_{12} & D_{12} & & & \\ D_{12} & D_{11} & D_{12} & & 0 & \\ D_{12} & D_{12} & D_{11} & & & \\ & & & D_{44} & 0 & 0 \\ & 0 & & 0 & D_{44} & 0 \\ & & & 0 & 0 & D_{44} \end{bmatrix} \tag{2}$$

where D_{11}, D_{12}, D_{44} are the material constants related to Young's modulus, Poisson's ratio and shear modulus, respectively. Then, the Young's modulus will be given in different loading directions, which are developed from stiffness matrix $\boldsymbol{D}$ in global coordinate system. Then, the Young's modulus in global system can be described as

$$E=\left[\frac{D_{11}+D_{12}}{(D_{11}+2D_{12})(D_{11}-D_{12})}+\left(\frac{1}{D_{44}}-\frac{2}{(D_{11}-D_{12})}\right)\right]\cdot\left(\alpha_1^2\beta_1^2+\alpha_1^2\gamma_1^2+\gamma_1^2\beta_1^2\right) \tag{3}$$

where E is the Young's modulus of single crystal (or the Young's modulus inside the grain) in different loading directions, and the specific definitions of α_1, β_1 and γ_1 refer to Ref.[24].

1.3 Elastic formulation inside GBIR

In order to establish the computational model of elastic properties inside the GBIR, Fig.3 shows the simplified schematic diagram of DS crystal considering the GBIR.

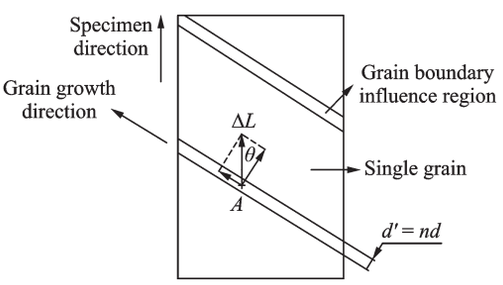

Fig. 3 Schematic diagram of DS superalloy considering GBIR

It is assumed that point A is an arbitrary point in the GBIR, and will produce small deformation when the load δF is used along the specimen direction. Due to the geometrical relationship shown in Fig.3, the deformation at point A can be decomposed into two parts: The deformation parallel and perpendicular to the grain growth direction, which can be expressed as

$$\begin{aligned}\Delta L_{A1}&=\Delta L_A\sin\theta\\ \Delta L_{A2}&=\Delta L_A\cos\theta\end{aligned} \tag{4}$$

where ΔL_{A1} and ΔL_{A2} are the deformation parallel and perpendicular to the grain growth direction without the influence of grain boundaries, respectively; ΔL_A refers to the total deformation at point A without the influence of grain boundaries and θ the angle between specimen direction and grain growth direction. In the foundation of the first hypothesis, ΔL_{A1}^* and ΔL_{A2}^* are related to the deformation parallel and perpendicular to the grain growth direction with the influence of grain boundaries, respectively

$$\begin{aligned}\Delta L_{A1}^*&=f(T)\Delta L_{A1}=f(T)\Delta L_A\sin\theta\\ \Delta L_{A2}^*&=\Delta L_{A2}=\Delta L_A\cos\theta\end{aligned} \tag{5}$$

where $f(T)$ is a factor restricting the deformation along the direction which perpendiculars to the grain growth direction in the GBIR, T represents the temperature. In this paper, only room temperature is taken into account and other temperatures will be discussed in following studies. So $f(T)$ is always equal to a constant f. Then, combining Eq.(4) with Eq.(5), the deformation at point A with the influence of grain boundaries can be clarified as

$$\begin{aligned}\Delta L_A^*&=\Delta L_{A1}^*\sin\theta+\Delta L_{A2}^*\cos\theta=\\ &\Delta L_A(\cos\theta^2+f^*\sin\theta^2)\end{aligned} \tag{6}$$

where ΔL_A^* indicates the deformation at point A with the influence of grain boundaries. Meanwhile, we have

$$\sigma_A=E_A\frac{\Delta L_A}{L_A} \tag{7}$$

$$\sigma_A=E_A^*\frac{\Delta L_A^*}{L_A} \tag{8}$$

where σ_A is the equivalent stress along the specimen direction, and ΔL_A the length along the specimen direction of a tiny element at point A. E_A and E_A^* are the Young's modulus without and with the influence of grain boundaries, respectively. Obviously, combining Eq.(7) with Eq.(8), the Young's modulus inside the GBIR can be expressed as

$$E_A^*=\frac{E_A}{\cos\theta^2+f^*\sin\theta^2} \tag{9}$$

1.4 Establishment of GBE model of DS superalloys

The macroscopic equivalent elastic modulus along different tensile directions of DS superalloys is obtained from the Voigt and Reuss averages. Due to the second assumption, the width of the GBIR can be expressed as

$$d'=nd \tag{10}$$

where d' is the width of the GBIR and n the model parameter. Based on the Voigt and Reuss methods, we have

$$\overline{E}=\frac{E_{\text{Voigt}}+E_{\text{Reuss}}}{2} \tag{11}$$

where

$$E_{\text{Voigt}} = f_{V1}E_1 + f_{V2}E_2$$
$$\frac{1}{E_{\text{Reuss}}} = \frac{f_{V1}}{E_1} + \frac{f_{V2}}{E_2} \tag{12}$$

where $\overline{E}$ is the macroscopic equivalent modulus along the specimen direction of DS superalloys, E_{Voigt} and E_{Reuss} are the upper bound and the lower bound of the macroscopic equivalent modulus of DS superalloys, respectively. f_{V1} and f_{V2} are the volume fractions of the grain and the GBIR. E_1 and E_2 are the macroscopic equivalent modulus along the specimen direction in the grain and the GBIR, respectively.

The formulas used in the model are summarized as follows

$$\begin{cases} \overline{E} = \dfrac{E_{\text{Voigt}} + E_{\text{Reuss}}}{2} \\ E_{\text{Voigt}} = f_{V1}E_1 + f_{V2}E_2 \\ \dfrac{1}{E_{\text{Reuss}}} = \dfrac{f_{V1}}{E_1} + \dfrac{f_{V2}}{E_2} \end{cases}$$
$$E_1 = E_A = E = \left[\frac{D_{11} + D_{12}}{(D_{11} + 2D_{12})(D_{11} - D_{12})} + \left(\frac{1}{D_{44}} - \frac{2}{D_{11} - D_{12}}\right)\right] \cdot \left(\alpha_1^2\beta_1^2 + \alpha_1^2\gamma_1^2 + \gamma_1^2\beta_1^2\right)$$
$$E_2 = E_A^* = \frac{E_A}{\cos\theta^2 + f^* \sin\theta^2}$$
$$f_{V1} = \frac{(D - d')^2}{D^2}$$
$$f_{V2} = 1 - f_{V1}$$
$$d' = nd$$

There are total three parameters (f, n and d) in the model. d is the characteristic parameter of material determined by micro observations. f and n are the model parameters fitted by macro experimental results.

2 Comparison and Discussion

2.1 Experimental results

For the sake of validating GBE model, tensile testing experiments on IC10 DS have been taken along different axis-grain growth direction angles of the grains at ambient temperature. The nominal chemical composition weight percentage of IC10 DS, a directionally solidified Ni3Al-base superalloy commonly used for turbine blades, is listed in Table 1. There are total five groups of tests with the axis-grain growth direction angle, θ, chosen to be 0°, 22.5°, 45°, 67.5°, and 90°. The five kinds of tensile specimens are cut from a plate of IC10 DS as shown in Fig.4(a). Meanwhile, the dimensions of the experimental specimen are given in Fig.4(b). Detailed experimental procedures refer to GB/T 228—2002 (Metallic materials-tensile testing at ambient temperature).

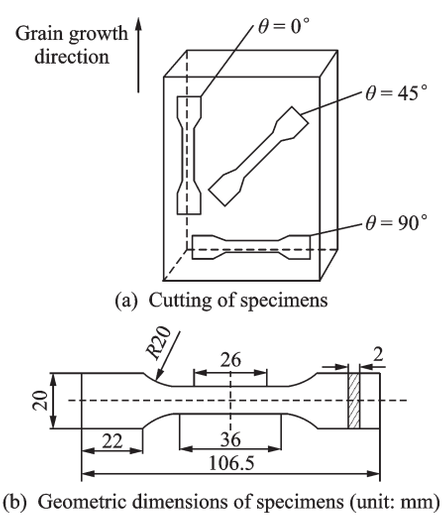

(a) Cutting of specimens

(b) Geometric dimensions of specimens (unit: mm)

Fig.4 Schematic diagrams of the tensile specimens

Table 1 Nominal chemical composition of IC10 DS superalloy (in weight) %

Element	C	Cr	Co	W	Mo	Al	B	Ta	Hf	Ni
Min	0.07	6.5	11.5	4.8	1.0	5.6	0.01	6.5	1.3	Bal.
Max	0.12	7.5	12.5	5.2	2.0	6.2	0.02	7.5	1.7	Bal.

The experimental results of monotonic tensile tests on IC10 DS superalloy are given in Fig.5(a). The measured Young's moduli obtained from the experimental results are listed in Table 2. The experimental results show that the minimum measured value is found at $\theta = 0°$, and the Young's modulus increases with θ, reaching the maximum value at $\theta = 45°$. Then, a general decrease of the Young's

modulus happens when θ is larger than 45°. This tendency of Young's modulus along different tensile orientations of IC10 is similar to that of CM247LC DS, another type of DS superalloy, at 850 ℃[2]. Furthermore, Fig.5(b) shows the experimental results of IC10 DS and IC10 SC when $\theta=0°$, and it can be seen that the Young's modulus of IC10 DS is almost the same as that of IC10 SC. Thus, it is concluded that the grain boundaries have little effect on the Young's modulus for DS superalloy when $\theta=0°$.

Table 2 Young's moduli measured by experiments

θ/(°)	0	22.5	45	67.5	90
E/ GPa	125.72	177.49	256.0	192.00	144.97

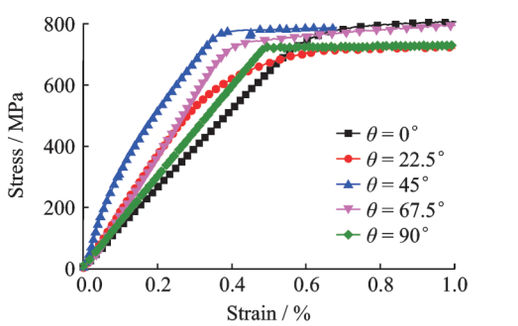

(a) Stress-strain curves of IC10 DS in different directions

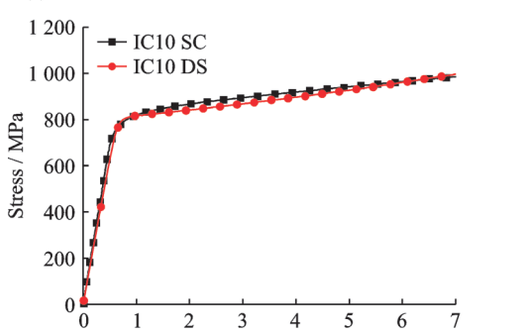

(b) Stress-strain curves when $\theta=0°$

Fig.5 Experimental stress-strain curves of IC10 superalloy

2.2 3D finite element simulations

In order to further verify the GBE model, 3D finite element (FE) simulation has been implemented. Representative volume element (RVE) has been simulated under different loading directions. All simulations are finished with a user material subroutine by ABAQUS.

According to the full scale of specimens, the size of RVE is chosen to be 150 μm×100 μm×600 μm, as shown in Fig.6. Meanwhile, the specimen direction coincides with z, one axis in the global coordinate system. During the simulation, element C3D10 is adopted and the mesh includes 17 865 elements. To emulate experimental conditions, a tensile constant strain rate is applied to the node $x=0$ μm, $y=0$ μm, $z=0$ μm. Moreover, all nodes in six surfaces of RVE subject to periodic boundary conditions[25].

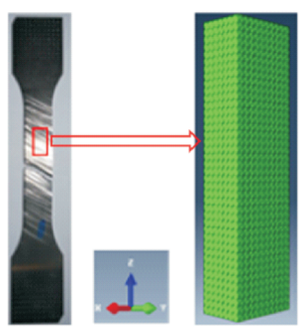

Fig.6 RVE of FE simulation

As reported previously, it is indicated that the grain growth direction in DS alloys is not exactly consistent with directionally solidified direction and the angle between them, Euler angle θ shown in Fig.3, obeys a Gaussian distribution. Thus, there are transgranular and intergranular misorientations of DS superalloys. In order to produce the microstructure of DS superalloys, all Gauss points in RVE are divided into different parts belong to different grains and the corresponding crystal orientation is attributed to each Gauss point. Detailed process is recorded in Ref.[5].

Fig.7 shows the typical FE contour plots of axi-

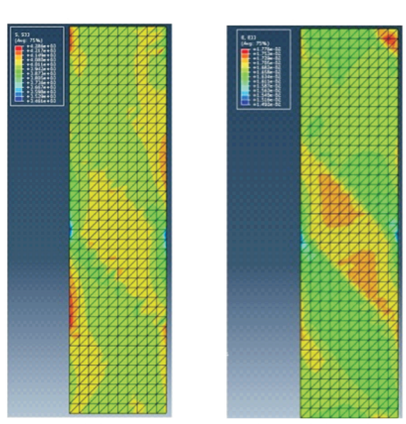

(a) Axial stress (b) Axial strain

Fig.7 Simulation results of axial stress and axial strain in a 3D FE model with $\theta=45°$

al stress and strain distributions in a RVE whose axis at 45° with respect to the grain growth direction. It is indicated that the stress and strain distributions in one grain are different to another which proves that grain boundaries have great influence on mechanical properties in DS superalloys. Young's moduli are acquired from the corresponding average stress-strain responses of the RVE and the predicted Young's moduli are shown in Table 3. Obviously, the tendency of the relationship between Young's modulus and tensile orientations is consisted with the experimental results shown above.

Table 3 Comparison of predicted Young's moduli by FE and experimental values

θ/(°)	0	22.5	45	67.5	90
Predicted value by FE/ GPa	135.0	179.36	251.60	191.20	133.0
Experimental value/ GPa	125.72	177.49	216.79	192.00	144.97

2.3 GBE model predictions

2.3.1 Young's modulus predicted by GBE model

There are seven constants in the GBE model: D_{11}, D_{12} and D_{44}, which are obtained from empirical formulae of SC[23], are elastic constants of single crystal; D and d are the dimension parameters in micro scale and they can be measured from Fig.8; f and n are the model parameters fitted from experimental results when θ is chosen to be 0°, 45°, and 90°. All constants are provided in Table 4 and the Young's moduli predicted by GBE model are given in Table 5. In Table 5, the predicted Young's moduli are in good agreement with experimental results, thus, the GBE model is effective in predicting Young's moduli of DS superalloy under different loading directions.

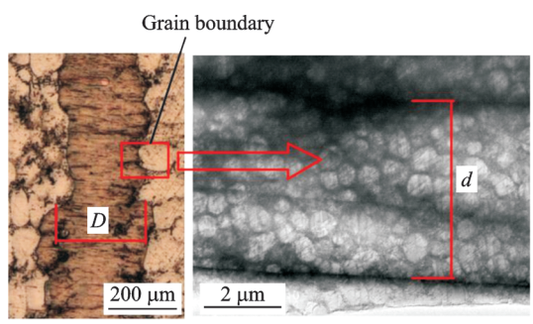

Fig.8 Optical microscope images of grains (left) and TEM images of grain boundaries (right) in IC10 DS superalloy

Table 4 Material parameters in the GBE model

Elastic constant			Dimension parameter		Model parameter	
D_{11}/ GPa	D_{12}/ GPa	D_{44}/ GPa	D/ μm	d/ μm	f	n
290.92	188.76	133.62	400	4.4	0.35	7

Table 5 Comparison of predicted Young's moduli by GBE model and experimental values

θ/(°)	0	22.5	45	67.5	90
Predicted value by GBE/ GPa	129.17	169.70	251.28	189.05	152.63
Experimental value/ GPa	125.72	177.49	216.79	192.00	144.97

Fig.9 shows the comparison results of different prediction methods and experiments. In Fig.9, it is indicated that the predicted Young's modulus by GBE model (labeled "Predicted results by GBE model") relates closely to the angle between the grain growth direction and the specimen axis, θ in Fig.2(b). Similarly, the predicted Young's modulus increases rapidly when $\theta < 45°$, however, decreases rapidly when $\theta > 45°$. The Young's modulus at $\theta = 0°$ is smaller than that at $\theta = 90°$. The above tendency is similar to that of the experimental and FE simulated results. The predicted Young's moduli obtained from empirical formulae of SC (labeled "Predicted results by SC model") are symmetric about a central line (the dash line in Fig.9), however, the Young's moduli predicted by GBE model and FE simulations are asymmetric. The predicted values by SC model are not in agreement with experimental results, especially when θ is larger than 45°. Moreover, when $\theta = 0°$, the Young's

moduli predicted by GBE model and SC model are almost the same, which is in accordance with the experimental results, as shown in Fig.5(b). To sum up, the GBE model and the FE simulation method can reflect the relationship between Young's modulus and loading directions for DS superalloys. Thus, the GBE model and the FE simulation method are more accurate than SC model. Simultaneously, compared with the FE simulation method, the GBE model is more simple, convenient and economical.

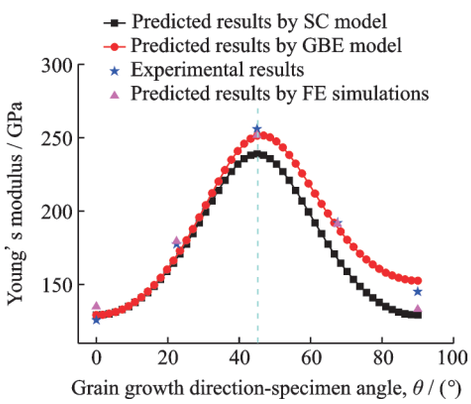

Fig. 9 Comparisons of experimental Young's moduli and calculated values by different methods

In order to analyze the rationality and necessity of the GBE model, error function is defined as $E_{\text{error}} = \dfrac{E_{\text{pre}} - E_{\text{exp}}}{E_{\text{exp}}}$, where E_{error} is the error value of Young's modulus, E_{pre} the prediction of Young's modulus, and E_{exp} the trial value of Young's modulus. Table 6 shows the error between trial value and predictions of Young's modulus. In Table 6, the Young's modulus predicted by the GBE model coincides well with experimental and FE simulated results. However, for SC model, the effects of grain boundary on deformation are not taken into consideration, thus, predictions are not exactly in agreement with the trial values, especially when $\theta = 67.5°$, and the error ups to -12.6%, which is unacceptable in engineering application.

2.3.2 Influence of f and n

f and n are two significant model parameters with explicit physical meanings in the GBE model. f represents the effects of grain boundaries on the deformation of DS superalloys and n the area size of grain boundaries influence region. Meanwhile, f and n are temperature-related variables. The relationship between f or n and the temperature will be discussed in successive research, and the temperature is 25 ℃ in current work. As shown in Fig.10, with the increase of f and n, the Young's modulus predicted by GBE model will raise and the asymmetry of the curves will also increase. The effects of the variety of f on predicted results are greater than that of n. To further determine the reasonable range of f and n, 3D stereogram has been given by MATLAB to

Table 6 Error between predicted and tested Young's moduli

θ/(°)	0	22.5	45	67.5	90
Experiment/ GPa	125.72	177.49	256.0	192.0	144.97
SC model/ GPa	129.17	167.74	238.89	167.74	129.17
Error/%	2.7	−5.5	−6.7	−12.6	−10.9
GBE model/ GPa	129.17	169.70	251.28	189.05	152.63
Error/%	2.7	−4.4	1.8	−1.5	5.3
FE simulation/ GPa	135.0	179.36	251.6	191.2	133.02
Error/%	7.4	1.1	1.7	−0.4	−8.2

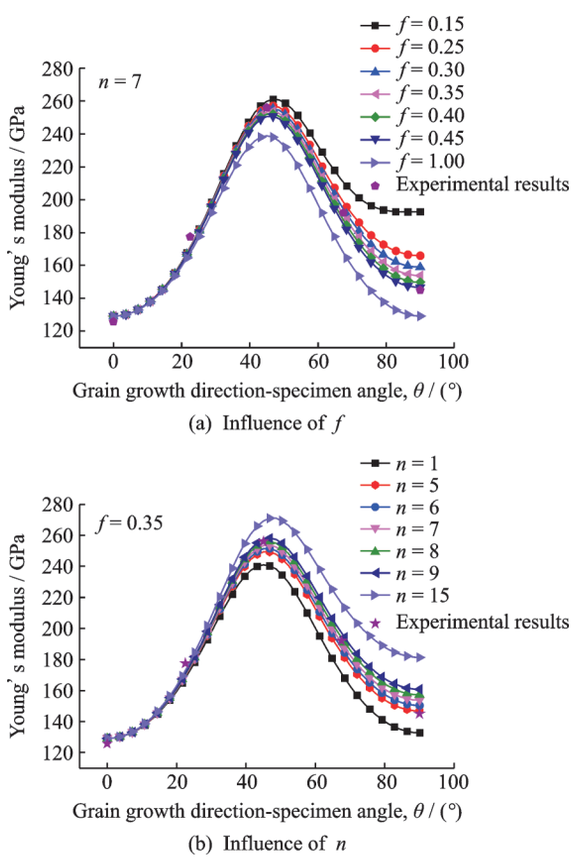

Fig.10 Influence of model parameters on prediction results

show the relationship between f, n, and Young's modulus in Fig.11. It is easily found in Fig.10 that the change of f and n has little influence on simulated results when θ is 0° and 22.5°. Thus, in Figs.11(a)—(c), only three cases (θ is 45°, 67.5°, and 90°, respectively) have been studied. In order to consider engineering errors, not only the experimental values planes but also the upper and the lower bound planes of errors are given in the three-dimensional graphs. Here, the maximum engineering error is set to be 5%. In Figs.11(a)—(c), f and n in the curves, the intersection lines between the simulated values planes and the upper and the lower bound planes of errors, are boundary values. In Fig.11(d), six curves under three conditions are projected into the XY plane. It is obvious that f and n in shadow area are reasonable for simulation. Thus, f is suggested to be 0.25—0.39 and n is 3—8.

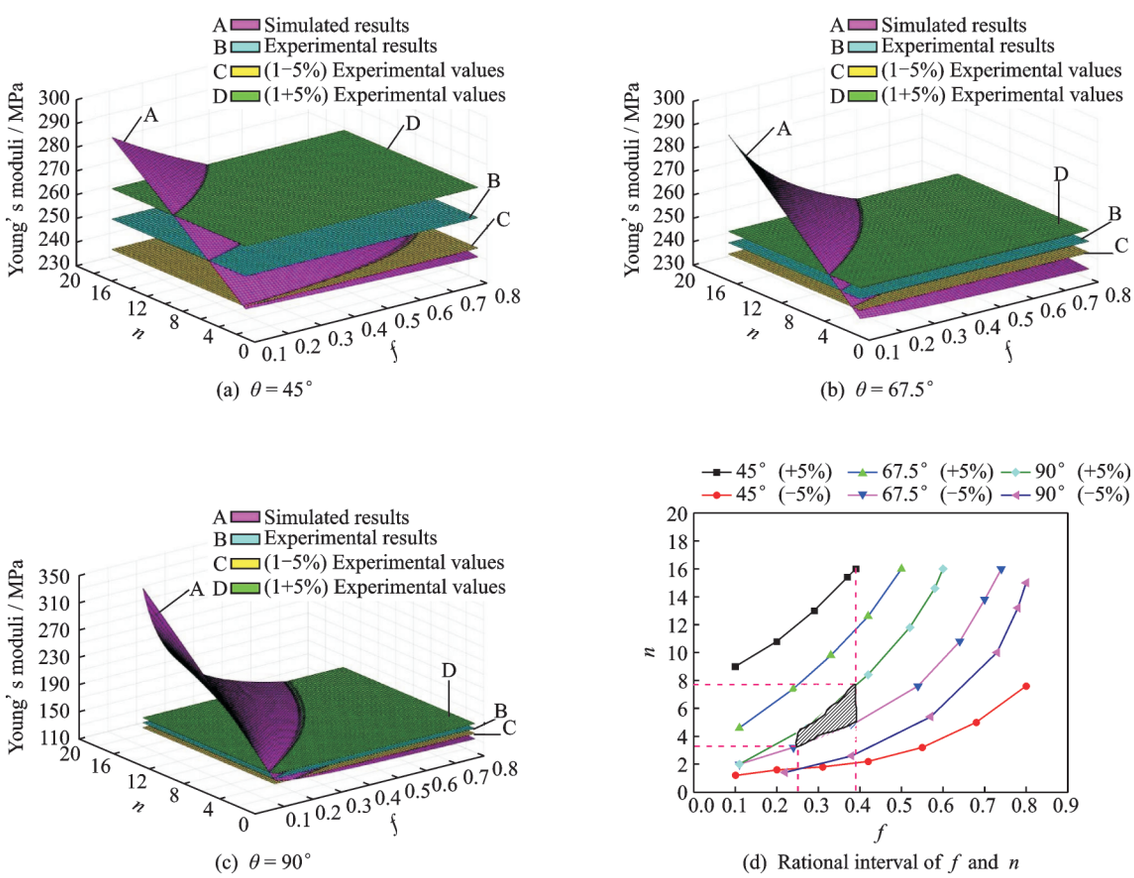

Fig.11 3D relationship plot of the relationship between f, n and Young's modulus when θ = 45°, 67.5°, 90°

3 Conclusions

Firstly, a GBE model is developed to predict the Young's modulus under different tensile orientations. The influence of grain boundaries and tensile orientations is taken into consideration directly in this model and the developed model is simple and convenient in engineering application.

Secondly, 3D finite element simulation and tensile experiments on a Ni3Al-base DS superalloy (IC10) along five orientations are carried out to verify the validity and the rationality of GBE model. Meanwhile, microscopic image technology is adopted to observe the grain boundaries. The predicted Young's modulus by GEB model is perfectly consistent with experimental and simulated results.

Lastly, the influence of two important parameters, f and n, in GBE model is studied. The results reveals that, for IC10 DS, f is suggested to be 0.25—0.39 and n is 3—8.

References

[1] ZHANG W G, LIU L, ZHAO X B, et al. Progress

in directionally solidified super alloys[J]. Foundary, 2009, 58(1): 1-6. (in Chinese)

[2] ROBERT A K. Thermomechanical fatigue behavior of the directionally-solidified nickel-base superalloy[D]. Atlanta: Woodruff School of Mechanical Engineering, 2008.

[3] SHENOY M. Constitutive modeling and life prediction in Ni-base superalloys[D]. Atlanta: Woodruff School of Mechanical Engineering, 2006.

[4] WHITESELL H S, OVERFELT R A. Influence of solidification variables on the microstructure, macro segregation, and porosity of directionally solidified Mar-M247[J]. Materials Science and Engineering A, 2001, 318(1/2): 264-276.

[5] YAGUCHI M, BUSSO E P. On the accuracy of self-consistent elasticity formulation for directionally solidified polycrystal aggregates[J]. International Journal of Solids and Structures, 2005, 42(3/4): 1073-1089.

[6] SHAHRIYAR K, SOMNATH G. Multi-scale crystal plasticity finite element model approach to modeling nickel-based superalloys[J]. Acta Materialia, 2013, 61(17): 6549-6561.

[7] WANG A J, KUMAR R S, SHENOY M M, et al. Microstructure-based multiscale constitutive modeling of γ-γ' nickel-base superalloys[J]. International Journal for Multiscale Computational Engineering, 2006, 4(5/6): 663-692.

[8] SHENOY M, TJIPTOWIDJOJO Y, Mcdowell D. Microstructure-sensitive modeling of polycrystalline IN 100[J]. International Journal of Plasticity, 2008, 24(10): 1694-1730.

[9] MISRA A, GIBALA R, NOEBE R D. Deformation and fracture behavior of a directionally solidified β/γ' Ni-30 At.Pct Al alloy[J]. Metallurgical and Materials Transactions A, 1999, 30(4): 1003-1015.

[10] ASTHANA R, TIWARI R, TEWARI S N. Compressive properties of zone-directionally solidified β-Ni3Al and its off-eutectic alloys with chromium and tungsten[J]. Materials Science and Engineering A, 2002, 336(1/2): 99-109.

[11] BEI H, GEORGE E P. Microstructure and mechanical properties of a directionally solidified NiAl-Mo eutectic alloy[J]. Acta Materialia, 2005, 53(1): 69-77.

[12] SAI K, CAILLETAUD G, FOREST S. Micro-mechanical modeling of the inelastic behavior of directionally solidified materials[J]. Mechanics of Materials, 2006, 38(3): 203-217.

[13] SHI D Q, DONG C L, YANG X G. Constitutive modeling and failure mechanisms of anisotropic tensile and creep behaviors of nickel-base directionally solidified superalloy[J]. Materials and Design, 2013, 45: 663-673.

[14] SHENOY M M, GORDON A P, MCDOWELL D L, et al. Thermomechanical fatigue behavior of a directionally solidified Ni-base superalloy[J]. Engineering Materials and Technology, 2005, 127(3): 325-336.

[15] MARTIN G, OCHOA N, SAI K, et al. A multiscale model for the elastoviscoplastic behavior of directionally solidified alloys: Application to FE structure computations[J]. International Journal of Solids and Structures, 2014, 51(5): 1175-1187.

[16] ZHANG H J, WEN W D, CUI H T. Behaviors of IC10 alloy over a wide range of strain rates and temperatures: Experiments and modeling[J]. Materials Science and Engineering A, 2009, 504(1/2): 99-103.

[17] ZHANG H J, WEN W D, CUI H T. An experimental study on constitutive equations of alloy IC10 over a wide range of temperatures and strain rates[J]. Materials and Design, 2012, 36: 130-135.

[18] CHEN L, WEN W D, CUI H T. Yielding description for a Ni3Al based intermetallic alloy[J]. Materials and Design, 2012, 41: 192-197.

[19] CHEN L, WEN W D, CUI H T. Generalization of Hill's yielding criterion to tension-compression asymmetry materials[J]. Science China Technological Sciences, 2013, 56(1): 89-97.

[20] ZHANG Hongjian. Research on the mechanical properties and constitutive equation of alloy IC10[D]. Nanjing: Nanjing University of Aeronautics and Astronautics, 2009. (in Chinese)

[21] HASEBE T, SAKANE M, OHNAMI M. Elastic anisotropy of directionally solidified superalloy[J]. Journal of Engineering Materials and Technology—Transactions of the ASME, 1992, 114(2): 141-146.

[22] ALLAN C D. Plasticity of nickel base single crystal superalloys[D]. Boston: Massachusetts Institute of Technology, 1997.

[23] LI S X, ELLISON E G, SMITH D J. The influence of orientation on the elastic and low cycle fatigue properties of several single crystal nickel base superaloys[J]. Journal of Strain Analysis for Engineering Design, 1994, 29(2): 147-153.

[24] BANDA G, NEMES J A. A new approach for single crystal materials analysis: Theory and application to initial yielding[J]. Journal of Engineering Materials

and Technology—Transactions of the ASME, 2005, 127(1): 119-129.

[25] XIA Z H, ZHANG Y F, ELLYIN F. A unified periodical boundary conditions for representative volume elements of composites and applications[J]. International Journal of Solids and Structures, 2003, 40(8): 1907-1921.

Acknowledgements The work was supported by the National Natural Science Foundation of China (No.51205190), the Fundamental Research Funds for the Central Universities (No.NS2016026), the Aeronautical Power Science Fund Project (No.6141B090317), and the Innovation Fund of Jiangsu Province, China (No.KYLX-0304).

Authors Mr. **XIAO Jianfeng** is currently a Ph.D. candidate at College of Energy and Power Engineering, Nanjing University of Aeronautics and Astronautics. His research field is the micro-mechanical behavior of superalloy materials.

Dr. **ZHANG Hongjian** graduated from the College of Energy and Power Engineering, Nanjing University of Aeronautics and Astronautics. His main research field is the mechanical behavior of advanced high temperature materials and composites.

Prof. **WEN Weidong** has been a professor at College of Energy and Power Engineering, Nanjing University of Aeronautics and Astronautics since 1985. His research focus is aerodynamic structure, strength and vibration.

Prof. **CUI Haitao** graduated from the mechanical design and theory in Northeast University in 1998. He has been working in College of Energy and Power Engineering, Nanjing University of Aeronautics and Astronautics since 1998. He is now a doctoral supervisor. His main research field is the mechanical properties of advanced aeroengine materials.

Author contributions Dr. **ZHANG Hongjian**, Prof. **WEN Weidong** and Prof. **CUI Haitao** designed the research direction and basic content. Additionally, Dr. **ZHANG Hongjian** and Prof. **CUI Haitao** gave important opinions on the writing of the paper. Mr. **XIAO Jianfeng** completed the establishment of the model, verification of the model, analysis of the model and writing of the paper.

Competing interests The authors declare no competing interests.

(Production Editor: Xu Chengting)